Aucubin alleviates oxidative stress and inflammation via Nrf2-mediated signaling activity in experimental traumatic brain injury

Han Wang
Nanjing University Medical School Affiliated Nanjing Drum Tower Hospital
Xiaoming Zhou
East Region Military Command General Hospital
Lingyun Wu
Nanjing University Medical School Affiliated Nanjing Drum Tower Hospital
Guangjie Liu
Nanjing University Medical School Affiliated Nanjing Drum Tower Hospital
Weidong Xu
East Region Military Command General Hospital
Xiangsheng Zhang
Nanjing University Medical School Affiliated Nanjing Drum Tower Hospital
Yongyue Gao
Nanjing University Medical School Affiliated Nanjing Drum Tower Hospital
Tao Tao
Nanjing University Medical School Affiliated Nanjing Drum Tower Hospital
Yan Zhou
Nanjing University Medical School Affiliated Nanjing Drum Tower Hospital
Yue Lu
Nanjing University Medical School Affiliated Nanjing Drum Tower Hospital
Juan Wang
Nanjing University Medical School Affiliated Nanjing Drum Tower Hospital
Chulei Deng
East Region Military Command General Hospital
Zong Zhuang
Nanjing University Medical School Affiliated Nanjing Drum Tower Hospital
Chunhua Hang
Nanjing University Medical School Affiliated Nanjing Drum Tower Hospital
Wei Li (lwxzlw@126.com)
Nanjing University Medical School Affiliated Nanjing Drum Tower Hospital https://orcid.org/0000-0002-9258-3500

Research

Keywords: Traumatic brain injury (TBI), Aubucin, Oxidative stress, Inflammation, Nuclear factor erythroid-2 related factor 2 (Nrf2)

Posted Date: February 25th, 2020

DOI: https://doi.org/10.21203/rs.2.24391/v1

Version of Record: A version of this preprint was published on June 15th, 2020. See the published version at https://doi.org/10.1186/s12974-020-01863-9.

Abstract

Background: Aucubin (Au) has anti-oxidative and anti-inflammatory bioactivities; however, its effects on a traumatic brain injury (TBI) model remain unknown. We explored the potential role of Au in a H_2O_2-induced oxidant damage in primary cortical neurons and weight-drop induced-TBI in a mouse model.

Methods: Neuronal apoptosis, brain water content, histological damages and neurological deficits and cognitive functions were measured. We performed western blot, TdT-mediated dUTP Nick-End Labeling (TUNEL) staining, Nissl staining, quantitative real time polymerase chain reaction (q-PCR), immunofluorescence/immunohistochemistry and enzyme linked immunosorbent assay (ELISA). RNA interference experiments were performed to determine the effects of Nuclear factor erythroid-2 related factor 2 (Nrf2) on TBI mice with intraperitoneal injection of Au.

Results: We found that Au enhanced the translocation of Nrf2 into the nucleus, activated antioxidant enzymes, suppressed excessive generation of reactive oxygen species (ROS) and reduced cell apoptosis in vitro and vivo experiments. In the mice model of TBI, Au markedly attenuated brain edema, histological damages and improved neurological and cognitive deficits. Au significantly suppressed high mobility group box 1(HMGB1)-mediated aseptic inflammation. Nrf2 knockdown in TBI mice blunted the antioxidant and anti-inflammatory neuroprotective effects of the Au.

Conclusions: Taken together, our data suggest that Au provides a neuroprotective effect in TBI mice model by inhibiting oxidative stress and inflammatory responses; the mechanisms involve triggering Nrf2-induced antioxidant system.

Introduction

Traumatic brain injury (TBI) is a major public health problem in modern society, causing functional impairments and imposing heavy economic burdens to patients. The pathophysiology of TBI consists of primary and secondary brain injuries[1, 2]. Trauma-induced primary brain injury results in tissue damage and neuronal loss. Secondary brain injury occurs hours or days following primary brain injury and involves glutamate excitotoxicity, neuroinflammation, calcium overload, oxidative stress and cell death[3]. Of these, oxidative stress and inflammatory reaction are recognized as the important pathobiological features of secondary brain damage[4, 5]. Excessive production of free radicals leads to lipid peroxidation, protein degradation, and genotoxicity leading to cellular and tissue damage[6]. Unfortunately, brain is an organ with a high content of polyunsaturated fatty acids, which makes it vulnerable to free radical attack and lipid peroxidation[7]. In addition, OS damage to mitochondrial function can collapse the cellular bioenergetics leading to cell apoptosis[6]. These OS-induced damaged cells released damage associated molecular patterns (DAMPs; e.g. ATP, RNA, high mobility group box-1) to initiate or exacerbate neuroinflammation. And the inflammatory respond also promotes ROS generation[8, 9]. Extensive animal data suggest that elevated antioxidant response and reduced inflammation would attenuate brain damage[10-12].

Nuclear factor erythroid-2 related factor 2 (Nrf2) has considerable neuroprotective effects in central nervous system (CNS) diseases[13-15]. Nrf2 is a transcription factor that takes part in regulation of cellular response to oxidative stress. Under normal physiological conditions, Kelch-like ECH-associated protein 1 (Keap1) combines with Nrf2 and enhances Nrf2 degradation. Once stimulated, Nrf2 translocates into the nucleus and binds to the antioxidant response element (ARE) in the promoter of antioxidant genes, thereby inducing the expression of antioxidant and detoxification enzymes and downstream proteins such as heme oxygenase-1 (HO-1), NAD(P)H: quinone oxidoreductase-1 (NQO-1), glutathione peroxidase (GPx), glutathione-S-transferase (GST) and superoxide dismutase (SOD)[16-18].

High-mobility group box 1 (HMGB1) is a member of DAMPs, which instigates and amplifies the noninfectious inflammatory response following TBI [19]. After secretion by inflammatory cells and/or expulsion by damaged neurons into the extracellular milieu [20, 21], HMGB1 interacts with Toll-like receptors (TLRs) on the microglia to initiate an immune response that actives myeloid differentiation factor 88 (MyD88) leading to translocation of nuclear factor-κB (NF-κB) dimers to the nucleus, where it binds to specific DNA sequences and promotes the transcription of inflammatory cytokine gene[22-24].

Aubucin is a member of the iridoid glycoside family. And it is widely distributed in plant species. Several lines of evidence suggest that Au has a wide range of pharmacological properties including antioxidation, anti-aging, anti-inflammation, anti-fibrosis, anti-tumor and hepatoprotection [25]. Recently, its anti-inflammatory and antioxidative functions have become a focus of research. Studies have shown that Au provides neuroprotective effects via anti-inflammation and anti-oxidative properties [26-30]. Nevertheless, its molecular mechanisms are not well understood. Recent reports have found that Au both exerts antioxidant and anti-inflammation properties by activating the Nrf2 signaling pathway in non-central nervous system diseases [31, 32]. However, to date, it remains unknown as to whether Au has the same protective effects on TBI. Therefore, we investigated the effects of Au on the secondary brain injury in an experimental mouse TBI model began to explore potential molecular mechanisms.

Materials And Methods

Animals

Pregnant C57BL/6 mice at 16–18 days' gestation and adult male C57BL/6 mice were purchased from the Animal Center of Drum Tower Hospital, Nanjing, China. All adult male C57BL/6 mice (25-30g) were raised in a 12-h light/dark cycle environment with free access to food and water.

Experiment design

Experiment 1

A total seven pregnant mice were used in the in vitro experiment. The primary cortical neurons were randomly assigned into five groups: Sham group, H_2O_2 group, H_2O_2 + Au group (50 μg/ml, 100 μg/ml, 200 μg/ml) for protein extraction (n = 3 for each group). In addition, three groups of neurons (Sham

group, H_2O_2 group, H_2O_2 + Au 200 μg/ml group) were used for immunofluorescence staining and ROS activity analysis (n = 3 for each group).

Experiment 2

We used 120 mice (130 mice underwent the operation, 120 survived). The mice randomly allocated into four groups: Sham group, TBI group, TBI + Au group (20 mg/kg and 40 mg/kg). We performed modified Neurological Severity Scores (mNSS), rotarod test, and Morris Water Maze (MWM) test (n = 8 for each group). The other mice were sacrificed on day 3 after trauma to measure brain water content (BWC) (n = 6 for each group).

Experiment 3

A total of 96 mice (107 mice underwent the operation, 96 survived) were randomly assigned to four groups: Sham group, TBI group, TBI + Au group (20 mg/kg and 40 mg/kg). All mice in this experiment were sacrificed at 3 d after trauma. Six mice in each group were used for western blot (WB), quantitative real time polymerase chain reaction (q-PCR) and enzyme linked immunosorbent assay (ELISA). Brain tissue from the remaining mice were used to make paraffin slices for TdT-mediated dUTP Nick-End Labeling (TUNEL) staining, Nissl staining, immunofluorescence (IF) staining and immunohistochemistry (IHC) staining (n = 6 for each group).

Experiment 4

First, 48 mice (56 mice underwent the operation, 48 survived) were divided into four groups (n = 6, each group): Sham group, TBI group, TBI + negative control (NC) group and TBI + lentiviral vectors (LV) group and were sacrificed at 3 d after TBI for WB and q-PCR to verify the effectiveness of the Nrf2-specific shRNA. Then, 30 mice (35 mice underwent the operation, 30 survived) were randomly assigned to five groups (n = 6, each group): Sham group, TBI group, TBI + Au group, TBI + Au + NC group and TBI + Au + LV group for WB.

Primary cortical neuron culture

Primary cortical neuron culture was performed as previously described[33]. Briefly, the skull, blood, meninges and hippocampus were carefully removed from the fetal mice brain. After cortical tissue digested within 0.25% trypsin for 5 min at 37 °C, the suspensions were passed through filters with 22 μm mesh size and were centrifuged at 1500 rpm for 5 min. The supernatant were discarded and the pellets were resuspended in neurobasal medium supplemented with streptomycin, penicillin, HEPES, glutamate and B27. The cells were distributed in poly-D-lysine-coated plates. We refreshed half of the medium every 2 days. After 7- 8 days culture, neurons were used in vitro experiments.

In vitro and in vivo model establishment

For in vitro studies, the primary cortical neurons were incubated with H_2O_2 dissolved in neuronal culture medium at a final concentration of 100μM for 12 hours according to published research with minor modification[34]. Then, the neurons were collected for WB, IF staining and ROS activity analysis. For in vivo experiments, we used the TBI model described above [11]. In brief, mice were anesthetized and then placed onto the platform of the weight-drop apparatus. After disinfection, mice scalps were cut with a longitudinal midline incision to expose the skull. Then, the weight-drop device with a 200 g was released from a height of 2.5 cm, to cause focal trauma on the hemisphere 1.5 mm lateral to the midline on the mid-coronal plane. Mice with scalp incisions were sutured and returned to their cages and awaked from anesthesia. Mice in the Sham group underwent the same procedures except for the weight drop.

Drug administration

For in vitro studies, Au was dissolved in neuronal culture medium at concentrations of 50 μg/ml, 100 μg/ml, or 200 μg/ml. After stimulating cells with H_2O_2, the various concentrations of Au were added immediately and given again at intervals of six hours. For in vivo studies, Au was dissolved in normal saline to reach final concentrations of 4 mg/ml. The intraperitoneal injection of Au (20 mg/kg or 40 mg/kg) were at 30min, 12h, 24h and 48h after TBI. In the RNA interference experiments, the mice were intraperitoneally injected with Au at 40 mg/kg.

Preparation of paraffin-embedded sections

Anesthetized mice were perfused 0.85% saline solution followed by 4% paraformaldehyde and the brain tissues were removed. After immersion in 4% paraformaldehyde for 24h, the brain tissues were dehydration and vitrification, then made into paraffin blocks, that were cut into 6 μm sections. After dewaxing and antigen repair, sections were used for IF staining, Nissl staining, TUNEL staining and IHC staining.

WB analysis

The neurons and brain tissue were collected for WB analysis. The procedure of nuclear and total protein extraction was performed as previously described[11]. Equal protein amounts were separated using polyacrylamide gel electrophoresis and transferred to polyvinylidene difluoride membranes blocked in 5% skim milk for 2 hours at indoor temperature. Then, the membranes were incubated with primary antibodies against Nrf2 (1:1000), H3 (1:5000), NQO-1 (1:1000), HO-1 (1:1000), B-cell lymphoma-2 (Bcl2, 1:200), Bcl-2 Associated X Protein (Bax, 1:200), cleaved-caspase 3 (CC3, 1:1000), matrix metalloprotein-9 (MMP-9, 1:1000), GPx1 (1:1000), SOD1 (1:200), Iba-1 (1:1000), HMGB1 (1:100), TLR4 (1:200), MyD88 (1:200), NF-κB p65 (1:1000), inducible Nitric Oxide Synthase (iNOS, 1:1000), Cyclooxygenase-2 (COX2, 1:500), Interleukin-1β (IL-1β, 1:500) or β-actin (1:3000) overnight at 4 °C. After washing 3 times for 15 min with Tris-buffered saline with Tween 20, the membranes were incubated with corresponding HRP conjugated secondary antibodies (1:5000) for 1 h at room temperature. The protein bands were detected using enhanced chemiluminescence (ECL). ImageJ software were used to measure the optical density of protein bands.

IF staining

The brain sections with antigen retrieval or cultured cells were treated with blocking buffer for 30 min at room temperature and then incubated with primary antibodies against Nrf2 (1:100), MAP2 (1:200), NeuN (1:200) and Iba-1 (1:100) overnight at 4 °C. The cells or slides were incubated with corresponding secondary antibodies Alexa Fluor 594 and/or Alexa Fluor 488 after washed in phosphate buffered saline-Tween twice for 20 min and counterstained with 4,6-diamidino-2-phenylindole (DAPI) for 5 minutes. Fluorescence was captured on a Zeiss HB050 inverted microscope system.

ROS detection

The procedures of ROS measurement were performed as described previously[35]. The H_2O_2-induced neurons were incubated with M29,79-dichlorodihydrofluorescein diacetate (DCFH-DA) for 10 min at 37 °C. The pictures were captured using an inverted fluorescence microscope. The mean fluorescence intensity was analyzed using ImageJ software.

IHC staining

The sections were incubated with primary antibodies against HO-1 (1:200), NQO1 (1:200) and 8-hydroxyguanosine (8-OHdG) (1:200) overnight at 4 °C after blocking for 30 min. The slides were washed twice with phosphate-buffered saline (PBS) and incubated with biotinylated secondary antibody and horseradish peroxidase (HRP)-streptavidin reagent. Then, the sections were re-stained with hematoxylin and we measured immunoreactivity using 3,3-diaminobenzidine (DAB). Images were pictured by a microscope. ImageJ software was used to analyze the IHC images.

Brain water content

The brain water content was performed at 3 d after TBI. The entire brain was divided into hemispheres, cerebellum and brainstem. Each part was weighed immediately to obtain the wet weight. Brain tissue was dried at 80 °C for 72 h and re-weighed again to calculate dry weight. The brain water content was calculated as [(wet weight – dry weight)/wet weight] ×100%.

Neurologic function testing

The mice were assessed using mNSS test on days 1 and 3 after TBI according to our previous studies[33]. The mNSS consists of motor (muscle status and abnormal movement), sensory (visual, tactile and proprioceptive), reflex, and balance tests. The higher score represents the more serious neurological impairment.

MWM test

On the 24^{th} day after the trauma, the mice were administered the MWM test with minor modifications to assess their cognitive functions based on previous experiments[36]. Visual cues of figures were hung on

the wall of the tank. During the acquisition phase, the mice were trained to find a submerged platform 1 cm below the surface of the water. The mice subjected to the probe trials on next day after 5 consecutive training days. The platform was removed from the tank, and then mice were placed in the quadrant opposite the platform. The ANY-Maze video tracking system was used to videotape the whole process and data.

Rotarod test

Mice were received three days of rotarod test training before TBI induction and then placed in a neutral position on an accelerating rotating rod (from 5 to 40 r/min within 5 min). The blinded experimenters recorded the latency to fall of each mouse. An average latency of three trials in one day represented the mouse motor performance. The test was performed before TBI and 0, 3, 7 and 14 days following TBI.

TUNEL staining and Nissl staining

TUNEL staining was performed as described previously[33]. In brief, antigen-repaired brain sections were incubated with TUNEL reaction mixture for 1 hours at room temperature. After washed two washes with PBS for 20 min, the slides were incubated with DAPI for 5 min. Then, the brain sections were washed twice again and exposed under an inverted fluorescence microscope. For Nissl staining, the sections were hydrated in 1% toluidine blue, washed with double-water and mounted with permount. The pictures were captured under a light microscope.

Contents of MDA, SOD, ROS, GSH and GSH-Px measurements

Levels of MDA, SOD, ROS, GSH and GSH-Px in serum and brain tissue were measured using ELISA kits according to the manufacturer's instructions at 3 d after TBI.

RNA interference

The transfection of LV expressing Nrf2-specific shRNA or negative control shRNA for mice brains in vivo were conducted according to previously described methods[36]. After induction of anesthesia, mice with scalp incisions were placed in a stereotaxic device, then a cranial burr hole (2.5 mm in depth, 1.2 mm lateral from midline, and 0.4 mm posterior from the bregma) was drilled. The mice underwent injection with 4 μL lentiviruses into the lateral ventricles (2 μL/min). The needle remained in place for 30 s after completing the infusion and the scalp incision was sutured. The mice in Sham, TBI and TBI + Au groups received a cranial burr hole, but not intracerebroventricular (ICV) injection. The experimental TBI was established 3 d after ICV injection. The Nrf2 shRNA sequence was 5'-AAGCCTTACTCTCCCAGTGAATCGAAATTCACTGGGAGAGTAAGGCTT-3' and a non-targeting RNA sequence serving as a negative control [37].

Quantitative real-time PCR

Q-PCR was performed as previously described[36]. Total mRNA was isolated from tissues using the Trizol reagent and measured using spectrophotometric analysis (OD260/OD280). After reverse transcription of total mRNA into cDNA, q-PCR analysis was performed with SYBR Green qPCR Master Mix. Nrf2 forward and reverse primers were 5′-CTACTCCCAGGTTGCCCACA -3′ and 5′-CGACTCATGGTCATCTACAAATGG-3′, respectively; HO-1 forward and reverse primers were 5'-GCTGGTGATGGCTTCCTTGTA-3' and 5'-ACCTCGTGGAGACGCTTTACAT-3', respectively; NQO-1 forward and reverse primers were 5'-ACGACAACGGTCCTTTCCAGA-3' and 5'-CAGAAACGCAGGATGCCACT-3', respectively; β-actin forward and reverse primers were 5′-GACAGGATGCAGAAGGAGATTACT-3′and 5′TGATCCACATCTGCTGGAAGGT-3', respectively. All samples were analyzed in triplicate with normalization to the β-actin in the Sham group. Relative quantification of mRNA expression was measured using the $2^{-\Delta\Delta CT}$ method.

Statistical analysis

The data were expressed as mean ± standard deviation (SD) and analyzed using an analysis of variance (ANOVA) followed by Tukey's (one-way) or Bonferroni's (two-way) multiple comparisons post-hoc test. Values of $p<0.05$ were considered statistically significant. Analyses were performed using SPSS version 20.0 software.

Results

Effects of Au on H_2O_2-induced primary cortical neurons

To determine the anti-oxidative effects of Au, we used H_2O_2 to stimulate primary neurons to construct a vitro model of oxidative stress. As shown in Figs. 1c and d, H_2O_2 significantly increased ROS levels when compared with those of the Sham group, and this effected was reversed by Au treatment. Western blot analysis showed that Au treatment significantly enhanced the cytoplasmic Nrf2 translocation to the nucleus and increased the expression of NQO-1, HO-1 and Bcl2 in a dose-dependent manner (Figs. 1a, b). In addition, western blot analysis also showed that Au reduced the expression of Bax and CC3 in neurons after H_2O_2 stimulation. Immunofluorescence staining were consistent with the western blot results that Au promoted the cytoplasmic Nrf2 into the nucleus in conditions of oxidative damage (Fig. 1e).

Au ameliorated brain edema and improved short-term neurologic functions after TBI

At 3 d after TBI, BWC increased significantly. Au treatment at 20 mg/kg and 40mg/kg alleviated brain edema (Fig. 2a). As shown in Figs. 2c, d, TBI caused the increased expression of the MMP-9 protein, which destroys the blood-brain barrier. But that was reversed by Au treatment. To further explore the neuroprotective effects of Au on TBI, we measured neurologic functions in the mice. Although Au therapy on the first day of trauma did not improve mNSS scores, it did improve significantly after three days of treatment (Fig. 2b). Furthermore, significantly greater recovery was observed in Au-treated TBI mice than in TBI mice as measured using the rotarod test (Fig. 2e).

Au improved long-term neurologic functions after TBI

During the training days (Fig. 2j) or the probe trials (Fig. 2k), there was no difference in average swimming speed among the four groups. However, TBI significantly caused the mice to show prolonged escape latency in the cued learning phase. By contrast, mice in TBI + Au groups had a shortened escape latency compared with those in the TBI group, suggesting that Au improved the learning functions in TBI mice (Fig. 2i). In the probe trial period, the TBI mice treated with Au had significantly greater correct quadrant dwell time (Fig. 2l) and more platform crossings (Fig. 2f, m) than did TBI mice, suggesting that Au improved memory functions in TBI mice.

Au promoted neurons survival after TBI

In the vivo studies, we also measured the expression of apoptosis-associated proteins, and western blot results were consistent with those in vitro. Au treated-TBI mice had significantly greater expression of Bcl2 and lower expression of Bax and CC3 than those of TBI mice (Figs. 3a, b). TUNEL staining showed that there were significantly more apoptotic positive cells in the TBI group than in TBI + Au group (Fig. 3c). Then, we measured damaged neurons in the ipsilateral cortex surrounding the injury site. As shown in Fig. 3d, the neurons were clear and intact in the Sham group. By contrast, damaged neurons displayed irregular cell bodies, shrinkage and hyperchromatic nuclei in significantly greater numbers in the TBI group. After Au administration, less neuron loss was found than in the TBI group.

Au attenuated oxidative stress after TBI

SOD, MDA, GSH and GSH-Px levels in serum and brain tissue were measured to determine whether Au suppressed TBI-induced oxidative damage. Both in serum and brain tissue, TBI significantly decreased SOD, GSH, and GSH-Px levels, whereas increased MDA levels. After Au application, mice in the TBI + Au groups (20 mg/kg or 40 mg/kg) displayed significantly higher serum levels and brain concentrations of SOD, GSH and GSH-Px than did TBI mice. Furthermore, mice with Au injection had significantly lower concentrations of serum and brain MDA than did those in the TBI group (Figs. 4a-d). Similarly, western blot results showed that the protein expression of SOD1 and GPx1 significantly increased in the TBI + Au groups as compared with those of the TBI group (Figs. 4e-g). In Figs. 4i, j, IHC staining was performed to determine whether Au treatment inhibited the production of the oxidative stress marker 8-OHdG. We found that Au treated-mice had significantly fewer 8-OHdG $^{+}$cells than did TBI mice.

Au promoted the expression and nuclear translocation of Nrf2 after TBI

WB analyses suggested that TBI significantly increased total and nuclear Nrf2 expression compared with that of the Sham group. TBI mice with Au treatment had further increased expression of total and nuclear Nrf2 (Figs. 5a, b, d). Meanwhile, cytoplasmic Nrf2 protein levels in TBI + Au groups were significantly lower than those of the TBI group (Figs. 5a, c). Immunofluorescence staining confirmed our WB findings that Au treatment enhanced Nrf2 nuclear translocation in neurons (Fig. 5e).

Au upregulated the expression of Nrf2 downstream proteins

We measured downstream pathway expression of Nrf2 at the mRNA and protein levels. Q-PCR results showed that TBI increased both *HO-1* and *NQO-1* mRNA, and Au further distinctly enhanced their expression in a dose-dependently (Figs. 6a, b). Consistent with mRNA variations, WB results demonstrated that Au caused greater protein expression of HO-1 and NQO-1 than in the TBI group (Figs. 6c, d). These results indicated that Au induced the expression of HO-1 and NQO-1 at the transcriptional and translational levels. In addition, representative immunohistochemical images of HO-1 and NQO-1 proteins are shown in Fig. 6e.

Au suppressed inflammatory response in the perilesional cortex after TBI

To measure microglial recruitment in the perilesional cortex, we used WB analyses and IF staining. The results showed that Au significantly weakened the increased expression levels of Iba-1 in the injured tissue (Fig. 7c). Representative IF images and WB bands of Iba-1 protein are respectively shown in Figs. 7a, b, respectively. Microglial activation is accompanied by morphological changes. Microglia from the TBI mice had enlarged, round cell bodies and shortened processes, while those in TBI + Au groups exhibited a less-activated phenotype with smaller cell bodies and elongated processes (Fig. 7a).

Then, we detected the expression of HMGB1 and downstream proteins. Au-treated mice had lower levels of HMGB1, TLR4, MyD88 and total NF-κB p65 than did TBI mice (Figs. 8a-c). Furthermore, NF-κB p65 in the nucleus were reduced in the TBI + Au group (Figs. 8a, c). There were consistent changes in inflammatory cytokines (Figs. 8d, e).

Nrf2 interference weakened the antioxidant and anti-inflammatory effects of Au on TBI

We wondered whether the neuroprotective effect of Au depended on Nrf2 activation after TBI. We applied Au (40 mg/kg) together with Nrf2 shRNA co-treatment. To test the effect of Nrf2 interference, q-PCR and WB analyses were performed. The results showed that Nrf2 shRNA significantly depressed expression of Nrf2 at the mRNA and protein levels (Figs. 9a-c). We further evaluated protein levels of nuclear Nrf2. Au and Nrf2 shRNA co-treated mice displayed a reduction in nuclear Nrf2 compared with that of the TBI + Au + NC group (Figs. 9d, f). Expression levels of HO-1 and Bcl2 were notably decreased in TBI + Au + LV groups, whereas Au-treated mice with Nrf2 interference showed increased protein expression of Bax and CC3 (Figs. 9d-f).

Finally, we measured expression of HMGB1 and TLR4 pathway components. The results indicated that Nrf2 knockdown significantly increased expression levels of HMGB1, TLR4, MyD88, nuclear NF-κB p65 and COX2 as compared with those of the TBI + Au + NC group (Fig.9g-i).

Discussion

Secondary brain injury has complex and varied pathophysiological mechanisms. Substantial evidence suggests that oxidative stress participates in secondary brain injury[4, 10, 11, 17]. Recently, studies have

demonstrated that Au has potent antioxidant effects and reduces excessive production of ROS in non-alcoholic fatty liver disease[31] and acute lung injury[32]. Until now, few experiments investigated the potential antioxidative in CNS diseases, except that Xue and colleagues reported the antioxidant bioactivities of Au in P12 cells (a neuronal cell line)[38, 39] and in a rat model of diabetic encephalopathy[27-29]. In the present study, we first investigated the antioxidative effects of Au on primary neurons. We found that Au inhibited intercellular ROS generation, restored the balance between the expression of Bcl2 and Bax and suppressed caspase-3 activation. These results are consistent with those of previous studies[27, 38]. Then, we further tested the effectiveness of Au in TBI mice. We found that Au administration substantially reduced MDA content and numbers of 8-OHdG-positive cells, which are markers of oxidative stress and indicate the presence of cellular damage and destruction[40]. Concomitant with the decreased generation of ROS, Au also increased brain and serum levels of essential antioxidant enzymes that inhibit the overproduction of ROS. These findings suggest that Au activates ARE to regulate cellular oxidant–antioxidant balance. TBI causes cerebral cortex damage that has been confirmed to affect a series of neurobehavioral functions[41]. In addition to motor deficits, TBI mice in our experiments exhibited cognitive impairments that were mitigated by Au treatment. This suggests that Au augments brain tissue repair and promotes functional recovery. Published literatures have shown that the neuroprotective effect of Au was both in the short term and the long term. The mechanisms involve in oxidative stress-induced neuronal loss[42]. After Au treatment, attenuation of oxidative stress could reduce neuronal loss in hippocampus[27-29]. Hence, we hypothesized that the improvement of neurologic functions in TBI mice was probably due to the fact that Au alleviated oxidative stress, leading to the reduced neuronal loss in the cortex and hippocampus.

Nrf2 plays an indispensable role in maintaining cellular homeostasis. Substantial lines of evidence have suggested that it is beneficial for CNS diseases, including TBI[13-15]. Under physiologic conditions, Nrf2 binds with Keap1 in the cytoplasm. However, under conditions of injury, Nrf2 dissociates from Keap1 and translocates into the nucleus, where it activates the Nrf2-ARE pathway. Au has been demonstrated to have the property to promote Nrf2 into nuclear, which triggers Nrf2-induced antioxidative signaling pathway[31, 32]. In both in vitro and vivo studies, we did find that Au enhanced nuclear accumulation of Nrf2 and increased cytoplasmic expression of HO-1 and NQO1 in neurons. While Nrf2 was down-regulated, the antiapoptotic and antioxidative properties were abrogated. These results indicate that Au ameliorated TBI in a Nrf2-dependent manner.

Inflammation is one of the major determinants of secondary brain damage after TBI[5]. Activated microglia, the principle resident macrophages of the CNS, produce and release a number of pro-inflammatory cytokines and chemokines. These cytokines activate and recruit more inflammatory cells to amplify the inflammatory response[43]. Au restrains the activation of astrocytes and microglia[26, 30]. Our results showed that Au inhibited the activation of microglia and prevented them from accumulating in the injury cortex. Moreover, we observed that Au markedly reduced protein levels of inflammatory cytokines. These findings suggest that Au also provides neuroprotective effects in a TBI model via anti-inflammation, whereas the anti-inflammatory role of Au was abrogated by Nrf2 knockdown. Consistent with these results, a recent study have showed that Nrf2 knockdown in RAW267.4 cells diminished the

bioactivity of Au to impede inflammation, indicating that Au-inhibited inflammation dependents on Nrf2 expression[32].

In TBI, there is crosstalk between oxidative and inflammation. ROS deplete cellular antioxidants, react with nucleotides and proteins and induce peroxidation of cellular membranes, further damaging cells and organelles, which initiates or intensifies inflammation[6, 8]. Damaged neurons and activated microglia passively and actively release HMGB1 into the extracellular milieu, respectively[20, 21]. HMGB1 binds with TLR4, a member of the TLR family, initiating the MyD88-dependent pathway leading to direct NF-κB activation and inducing the production of pro-inflammatory genes and chemokines[22-24]. A study has reported reduced expression of HMGB1 caused by Au treatment in epileptic mice[30]; however, the mechanism remains unclear. In the TBI model, our studies showed that Au inhibited HMGB1-TLR4 signaling pathway-mediated neuroinflammation, but this process relies on the expression of Nrf2. We hypothesize that attenuation of oxidative stress reduces the release of HMGB1, which alleviates the inflammatory response. Similarly, Zeng and Wang have reported that elevated antioxidant response reduces the inflammation and weakens the brain damage in the TBI model[10, 12].

There are several potential limitations deserving attention in our experiments. First, although studies have shown that Au plays a protective role by phosphorylating AMPK to regulate Nrf2 translocation into the nucleus[31, 32], we did not explore the specific molecular mechanism in TBI mice. Second, we only used Nrf2 shRNA to explore the mechanism, which might not have had an efficient inhibitor effect. Therefore, the data from Nrf2 knockout mice might be more persuasive.

Conclusions

In summary, we provide evidence that Aucubin has antioxidative and anti-inflammatory bioactivities in a TBI model. The underlying molecular mechanisms of these beneficial effects involve in regulation of ROS and HMGB1-mediated inflammation by trigger Nrf2-ARE signaling pathway. Our experimental results might provide a novel therapeutic strategy for TBI.

Abbreviations

Au: Aucubin; TBI: traumatic brain injury; TUNEL: TdT-mediated dUTP Nick-End Labeling; q-PCR: quantitative real time polymerase chain reaction; ELISA: enzyme linked immunosorbent assay; Nrf2: Nuclear factor erythroid-2 related factor 2; ROS: reactive oxygen species; HMGB1: high mobility group box 1; DAMPs: damage associated molecular patterns; CNS: central nervous system; Keap1: Kelch-like ECH-associated protein 1; HO-1: heme oxygenase-1; NQO-1: NAD(P)H: quinone oxidoreductase-1; GPx: glutathione peroxidase; GST: glutathione-S-transferase; SOD: superoxide dismutase; TLRs: Toll-like receptors; NF-κB: nuclear factor-κB; MyD88: myeloid differentiation factor 88; mNSS: modified Neurological Severity Scores; MWM: Morris Water Maze; BWC: brain water content; WB: western blot; IF: immunofluorescence; IHC: immunohistochemistry; NC: negative control; LV: lentiviral vectors; Bcl2: B-cell lymphoma-2; Bax: Bcl-2 Associated X Protein; CC3: cleaved-caspase 3; COX2: Cyclooxygenase-2; iNOS:

inducible Nitric Oxide Synthase; IL-1β: Interleukin-1β; ECL: enhanced chemiluminescence; DCFH-DA: M29,79-dichlorodihydrofluorescein diacetate; 8-OHdG: 8-hydroxyguanosine; ICV: intracerebroventricular

Declarations

Ethics approval and consent to participate

This study was approved by the Ethics Review Committee of Drum Tower Hospital.

Consent for publication

Not applicable

Availability of data and materials

All data during this study are included in this article.

Competing interests

The authors have no conflict of interest to disclose.

Funding

This work was funded by National Natural Science Foundation of China (NSFC) (No.81801166, No.81870922, No.81771291, No.81901203, No.81971127), the China Scholarship Fund (No.201606190196), the Fundamental Research Funds for the Central Universities (No.021414380361) and Medical Science and Technology Development Foundation, Nanjing Department of Health (No.JQX18001).

Authors' Contributions

Hang CH and Li W contributed to the design and analysis of the study and revised the manuscript; Wang H was responsible for performing experiments and manuscript drafting; Zhou XM and Wu LY were participated in creating the experimental animal model, drug administration and lentivirus injection; Liu GJ and Xu WD were responsible for WB and cell culture; Zhang XS and Gao YY were responsible for neurological evaluation and q-PCR; Tao T was responsible for IF staining and IHC staining; Zhou Y was responsible for ELISA and ROS detection; Lu Y was responsible for Nissl staining; Wang J was responsible for TUNEL staining; Deng CL was responsible for data collection; Zhuang Z was responsible for data analysis. All authors read and approved the final manuscript.

Acknowledgments

Not applicable

References

1. Lingsma HFM, Roozenbeek BM, Steyerberg EWP, Murray GDP, Maas AIM: Early prognosis in traumatic brain injury: from prophecies to predictions. *Lancet Neurology, The* 2010, 9:543-554.
2. Kuo C, Liou T, Chang K, Chi W, Escorpizo R, Yen C, Liao H, Chiou H, Chiu W, Tsai J: Functioning and Disability Analysis of Patients with Traumatic Brain Injury and Spinal Cord Injury by Using the World Health Organization Disability Assessment Schedule 2.0. *Int J Env Res Pub He* 2015, 12:4116-4127.
3. Sande A, West C: Traumatic brain injury: a review of pathophysiology and management. *J Vet Emerg Crit Car* 2010, 20:177-190.
4. Cornelius C, Crupi R, Calabrese V, Graziano A, Milone P, Pennisi G, Radak Z, Calabrese EJ, Cuzzocrea S: Traumatic brain injury: oxidative stress and neuroprotection. *Antioxid Redox Signal* 2013, 19:836-853.
5. Simon DW, McGeachy MJ, Bayir H, Clark R, Loane DJ, Kochanek PM: The far-reaching scope of neuroinflammation after traumatic brain injury. *Nat Rev Neurol* 2017, 13:572.
6. Sivandzade F, Prasad S, Bhalerao A, Cucullo L: NRF2 and NF-κB interplay in cerebrovascular and neurodegenerative disorders: Molecular mechanisms and possible therapeutic approaches. *Redox Biol* 2019, 21:101059.
7. Hall ED, Vaishnav RA, Mustafa AG: Antioxidant Therapies for Traumatic Brain Injury. *Neurotherapeutics* 2010, 7:51-61.
8. Eastman CL, D'Ambrosio R, Ganesh T: Modulating neuroinflammation and oxidative stress to prevent epilepsy and improve outcomes after traumatic brain injury. *Neuropharmacology* 2019:107907.
9. Forrester SJ, Kikuchi DS, Hernandes MS, Xu Q, Griendling KK: Reactive Oxygen Species in Metabolic and Inflammatory Signaling. *Circ Res* 2018, 122:877-902.
10. Wang J, Jiang C, Zhang K, Lan X, Chen X, Zang W, Wang Z, Guan F, Zhu C, Yang X, et al: Melatonin receptor activation provides cerebral protection after traumatic brain injury by mitigating oxidative stress and inflammation via the Nrf2 signaling pathway. *Free Radic Biol Med* 2019, 131:345-355.
11. Fang J, Wang H, Zhou J, Dai W, Zhu Y, Zhou Y, Wang X, Zhou M: Baicalin provides neuroprotection in traumatic brain injury mice model through Akt/Nrf2 pathway. 2018, Volume 12:2497-2508.
12. Zeng J, Chen Y, Ding R, Feng L, Fu Z, Yang S, Deng X, Xie Z, Zheng S: Isoliquiritigenin alleviates early brain injury after experimental intracerebral hemorrhage via suppressing ROS- and/or NF-κB-mediated NLRP3 inflammasome activation by promoting Nrf2 antioxidant pathway. *J Neuroinflamm* 2017, 14.
13. Liu L, Locascio LM, Dore S: Critical Role of Nrf2 in Experimental Ischemic Stroke. *Front Pharmacol* 2019, 10:153.
14. Calkins MJ, Johnson DA, Townsend JA, Vargas MR, Dowell JA, Williamson TP, Kraft AD, Lee JM, Li J, Johnson JA: The Nrf2/ARE pathway as a potential therapeutic target in neurodegenerative disease. *Antioxid Redox Signal* 2009, 11:497-508.

15. Zhang L, Wang H: Targeting the NF-E2-Related Factor 2 Pathway: a Novel Strategy for Traumatic Brain Injury. *Mol Neurobiol* 2018, 55:1773-1785.
16. Lv H, Liu Q, Zhou J, Tan G, Deng X, Ci X: Daphnetin-mediated Nrf2 antioxidant signaling pathways ameliorate tert-butyl hydroperoxide (t-BHP)-induced mitochondrial dysfunction and cell death. *Free Radic Biol Med* 2017, 106:38-52.
17. Ding K, Wang H, Xu J, Li T, Zhang L, Ding Y, Zhu L, He J, Zhou M: Melatonin stimulates antioxidant enzymes and reduces oxidative stress in experimental traumatic brain injury: the Nrf2-ARE signaling pathway as a potential mechanism. *Free Radic Biol Med* 2014, 73:1-11.
18. Wang J, Fields J, Zhao C, Langer J, Thimmulappa RK, Kensler TW, Yamamoto M, Biswal S, Dore S: Role of Nrf2 in protection against intracerebral hemorrhage injury in mice. *Free Radic Biol Med* 2007, 43:408-414.
19. Paudel YN, Shaikh MF, Chakraborti A, Kumari Y, Aledo-Serrano A, Aleksovska K, Alvim M, Othman I: HMGB1: A Common Biomarker and Potential Target for TBI, Neuroinflammation, Epilepsy, and Cognitive Dysfunction. *Front Neurosci* 2018, 12:628.
20. Yamada S, Maruyama I: HMGB1, a novel inflammatory cytokine. *Clin Chim Acta* 2007, 375:36-42.
21. Gao TL, Yuan XT, Yang D, Dai HL, Wang WJ, Peng X, Shao HJ, Jin ZF, Fu ZJ: Expression of HMGB1 and RAGE in rat and human brains after traumatic brain injury. *J Trauma Acute Care Surg* 2012, 72:643-649.
22. Miyake K: Innate immune sensing of pathogens and danger signals by cell surface Toll-like receptors. *Semin Immunol* 2007, 19:3-10.
23. Yang Y, Lv J, Jiang S, Ma Z, Wang D, Hu W, Deng C, Fan C, Di S, Sun Y, Yi W: The emerging role of Toll-like receptor 4 in myocardial inflammation. *Cell Death Dis* 2016, 7:e2234.
24. Lu Y, Zhang XS, Zhang ZH, Zhou XM, Gao YY, Liu GJ, Wang H, Wu LY, Li W, Hang CH: Peroxiredoxin 2 activates microglia by interacting with Toll-like receptor 4 after subarachnoid hemorrhage. *J Neuroinflammation* 2018, 15:87.
25. Zeng X, Guo F, Ouyang D: A review of the pharmacology and toxicology of aucubin. *Fitoterapia* 2020, 140:104443.
26. Zhu Y, Sun M, Jia X, Zhang P, Xu Y, Zhou Z, Xu Z, Cui C, Chen X, Yang X, Shen Y: Aucubin alleviates glial cell activation and preserves dopaminergic neurons in 1-methyl-4-phenyl-1,2,3,6-tetrahydropyridine-induced parkinsonian mice. *Neuroreport* 2018, 29:1075-1083.
27. Xue HY, Jin L, Jin LJ, Li XY, Zhang P, Ma YS, Lu YN, Xia YQ, Xu YP: Aucubin prevents loss of hippocampal neurons and regulates antioxidative activity in diabetic encephalopathy rats. *Phytother Res* 2009, 23:980-986.
28. Xue HY, Lu YN, Fang XM, Xu YP, Gao GZ, Jin LJ: Neuroprotective properties of aucubin in diabetic rats and diabetic encephalopathy rats. *Mol Biol Rep* 2012, 39:9311-9318.
29. Xue H, Jin L, Jin L, Zhang P, Li D, Xia Y, Lu Y, Xu Y: Neuroprotection of aucubin in primary diabetic encephalopathy. *Science in China Series C: Life Sciences* 2008, 51:495-502.

30. Chen S, Zeng X, Zong W, Wang X, Chen L, Zhou L, Li C, Huang Q, Huang X, Zeng G, et al: Aucubin Alleviates Seizures Activity in Li-Pilocarpine-Induced Epileptic Mice: Involvement of Inhibition of Neuroinflammation and Regulation of Neurotransmission. *Neurochem Res* 2019, 44:472-484.
31. Shen B, Zhao C, Wang Y, Peng Y, Cheng J, Li Z, Wu L, Jin M, Feng H: Aucubin inhibited lipid accumulation and oxidative stress via Nrf2/HO-1 and AMPK signaling pathways. *J Cell Mol Med* 2019, 23:4063-4075.
32. Qiu YL, Cheng XN, Bai F, Fang LY, Hu HZ, Sun DQ: Aucubin protects against lipopolysaccharide-induced acute pulmonary injury through regulating Nrf2 and AMPK pathways. *Biomed Pharmacother* 2018, 106:192-199.
33. Zhang X, Wu Q, Lu Y, Wan J, Dai H, Zhou X, Lv S, Chen X, Zhang X, Hang C, Wang J: Cerebroprotection by salvianolic acid B after experimental subarachnoid hemorrhage occurs via Nrf2- and SIRT1-dependent pathways. *Free Radic Biol Med* 2018, 124:504-516.
34. Singhal A, Morris VB, Labhasetwar V, Ghorpade A: Nanoparticle-mediated catalase delivery protects human neurons from oxidative stress. *Cell Death Dis* 2013, 4:e903.
35. Lu Y, Zhang X, Zhou X, Gao Y, Chen C, Liu J, Ye Z, Zhang Z, Wu L, Li W, Hang C: Peroxiredoxin 1/2 protects brain against H_2O_2-induced apoptosis after subarachnoid hemorrhage. *The FASEB Journal* 2019, 33:3051-3062.
36. Wang H, Zhou XM, Xu WD, Tao T, Liu GJ, Gao YY, Lu Y, Wu LY, Yu Z, Yuan B, et al: Inhibition of Elevated Hippocampal CD24 Reduces Neurogenesis in Mice with Traumatic Brain Injury. *J Surg Res* 2020, 245:321-329.
37. Lu C, Xu W, Shao J, Zhang F, Chen A, Zheng S: Nrf2 Activation Is Required for Ligustrazine to Inhibit Hepatic Steatosis in Alcohol-Preferring Mice and Hepatocytes. *Toxicol Sci* 2017, 155:432-443.
38. Xue HY, Niu DY, Gao GZ, Lin QY, Jin LJ, Xu YP: Aucubin modulates Bcl-2 family proteins expression and inhibits caspases cascade in H_2O_2-induced PC12 cells. *Mol Biol Rep* 2011, 38:3561-3567.
39. Xue HY, Gao GZ, Lin QY, Jin LJ, Xu YP: Protective effects of aucubin on H_2O_2-induced apoptosis in PC12 cells. *Phytother Res* 2012, 26:369-374.
40. Li Q, Han X, Lan X, Gao Y, Wan J, Durham F, Cheng T, Yang J, Wang Z, Jiang C, et al: Inhibition of neuronal ferroptosis protects hemorrhagic brain. *JCI Insight* 2017, 2:e90777.
41. Kragel PA, Kano M, Van Oudenhove L, Ly HG, Dupont P, Rubio A, Delon-Martin C, Bonaz BL, Manuck SB, Gianaros PJ, et al: Generalizable representations of pain, cognitive control, and negative emotion in medial frontal cortex. *Nat Neurosci* 2018, 21:283-289.
42. Zhao B: Natural antioxidants for neurodegenerative diseases. *Mol Neurobiol* 2005, 31:283-293.
43. Jassam YN, Izzy S, Whalen M, McGavern DB, El KJ: Neuroimmunology of Traumatic Brain Injury: Time for a Paradigm Shift. *Neuron* 2017, 95:1246-1265.

Figures

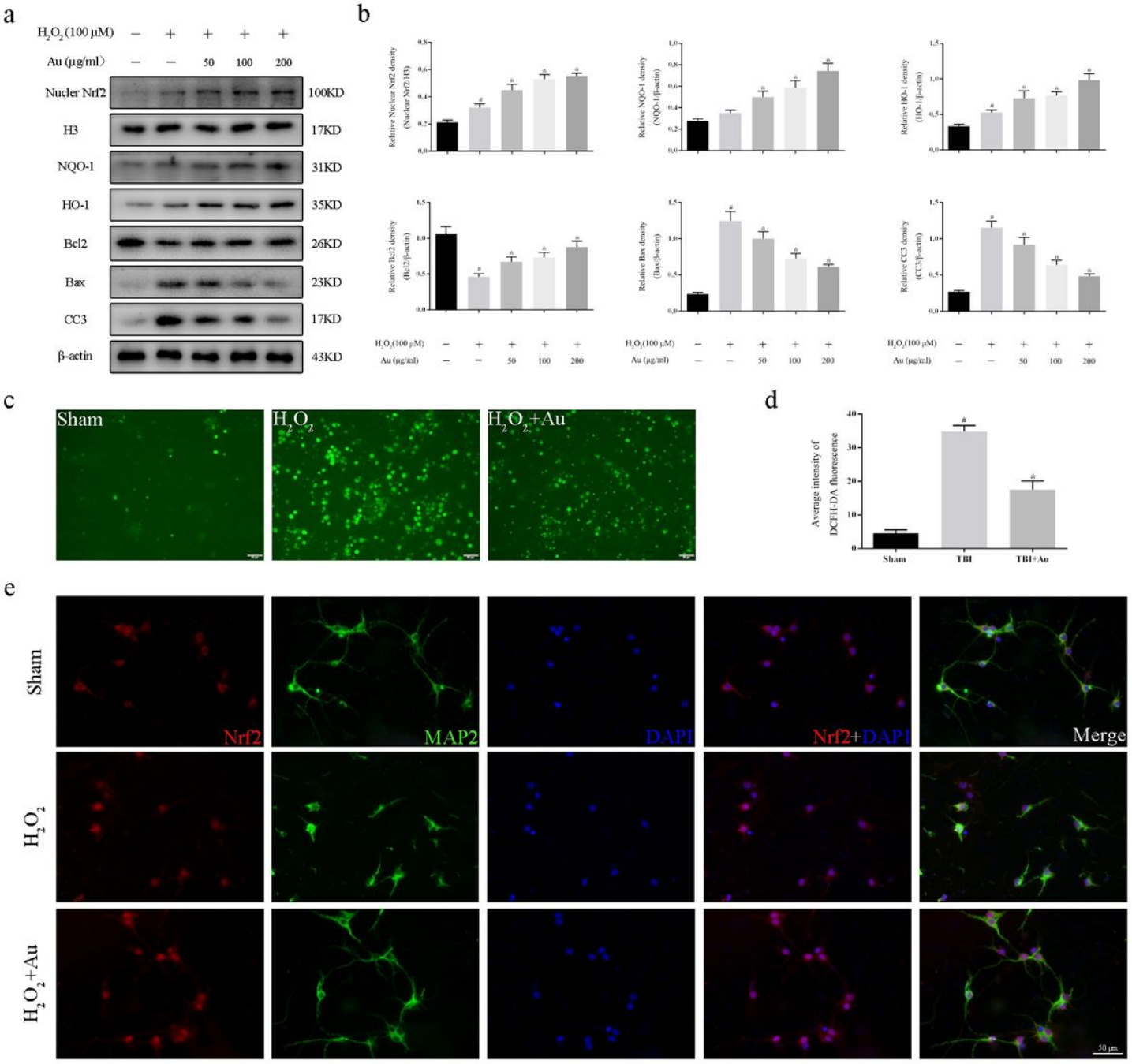

Figure 1

Effects of Au on the primary neurons exposed to 100μM H2O2. (a, b) Representative western blot bands (a) and quantification of relative protein expression (b) for nuclear Nrf2, NQO-1, HO-1, Bcl2, Bax and CC3. (c, d) Representative micrographs (c) and quantification (d) of DCFH-DA immunofluorescence in primary neurons. (e) Representative image of immunofluorescence staining for MAP2 and Nrf2. Bars represent the mean ± SD. #P < 0.05 versus Sham group; *P < 0.05 versus H2O2 group. Scale bars = 50 μm.

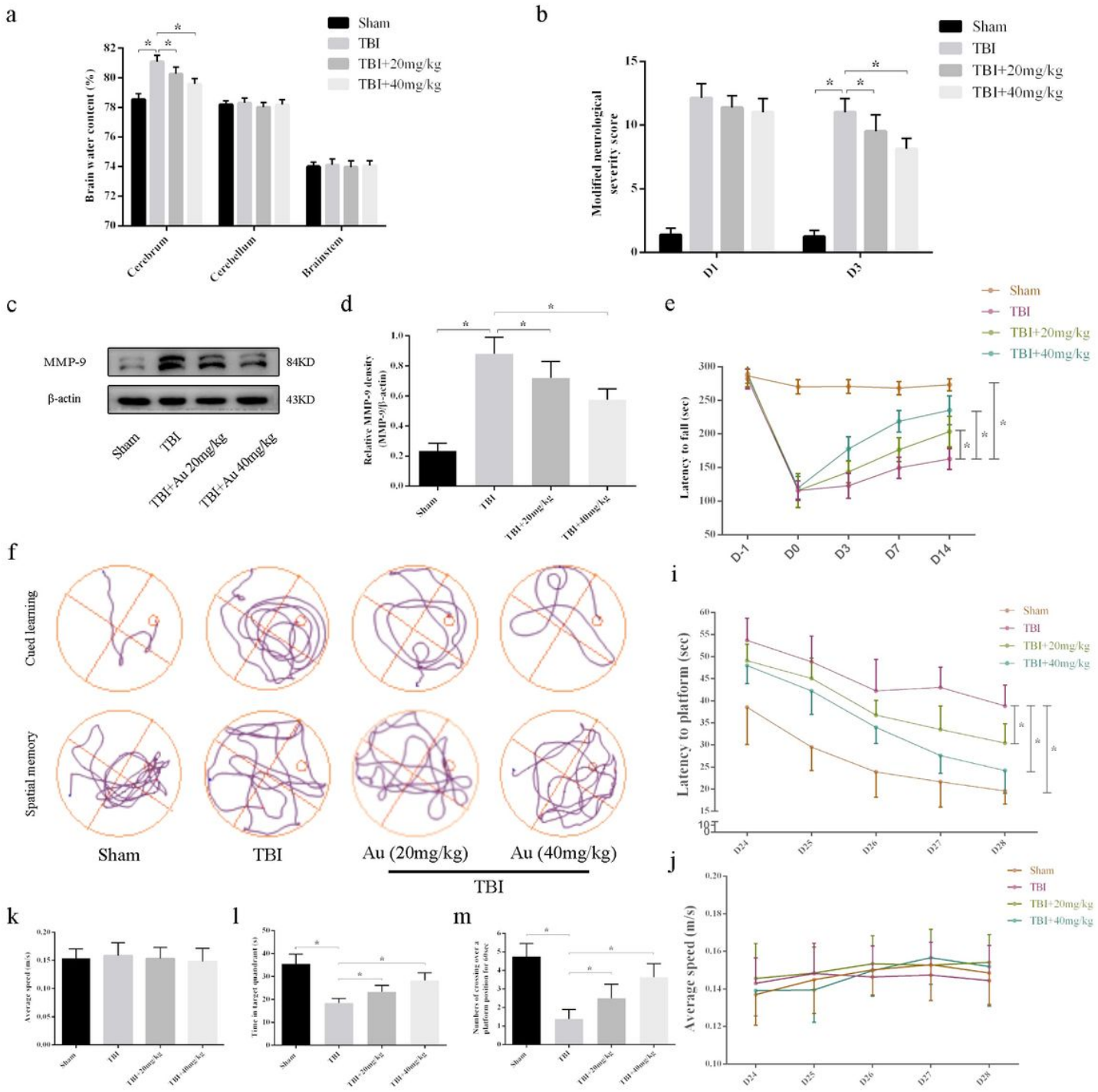

Figure 2

Au treatment reduced brain edema and improved neurologic functions. (a, b) Effects of TBI and Au on water content (a) and neurologic deficits (b). (c, d) Representative western blot bands (c) and quantification of relative protein expression (d) for MMP-9. (e) Effects of Au on the latency to fall in the rotarod test were analyzed using two-way ANOVA. The Bonferroni post hoc test was used to compare differences among several groups at 14 days post-TBI. (f) Typical swimming path of mice in all groups during the training days (upper) and the probe trial period (lower) of the MWM test. (i) Effects of Au on the latency to find platform in the MWM test. The two-way ANOVA was performed and the Bonferroni

post hoc test was utilized to compare differences among several groups on day 28. (j, k) Au did not affect the average swimming speed during the training days (j) or during the probe trial period (k). (l) Time spent in the correct quadrant during the probe trail. (m) Number of crossings over the platform position during the probe trail. Bars represent the mean ± SD. *P < 0.05 versus indicated groups.

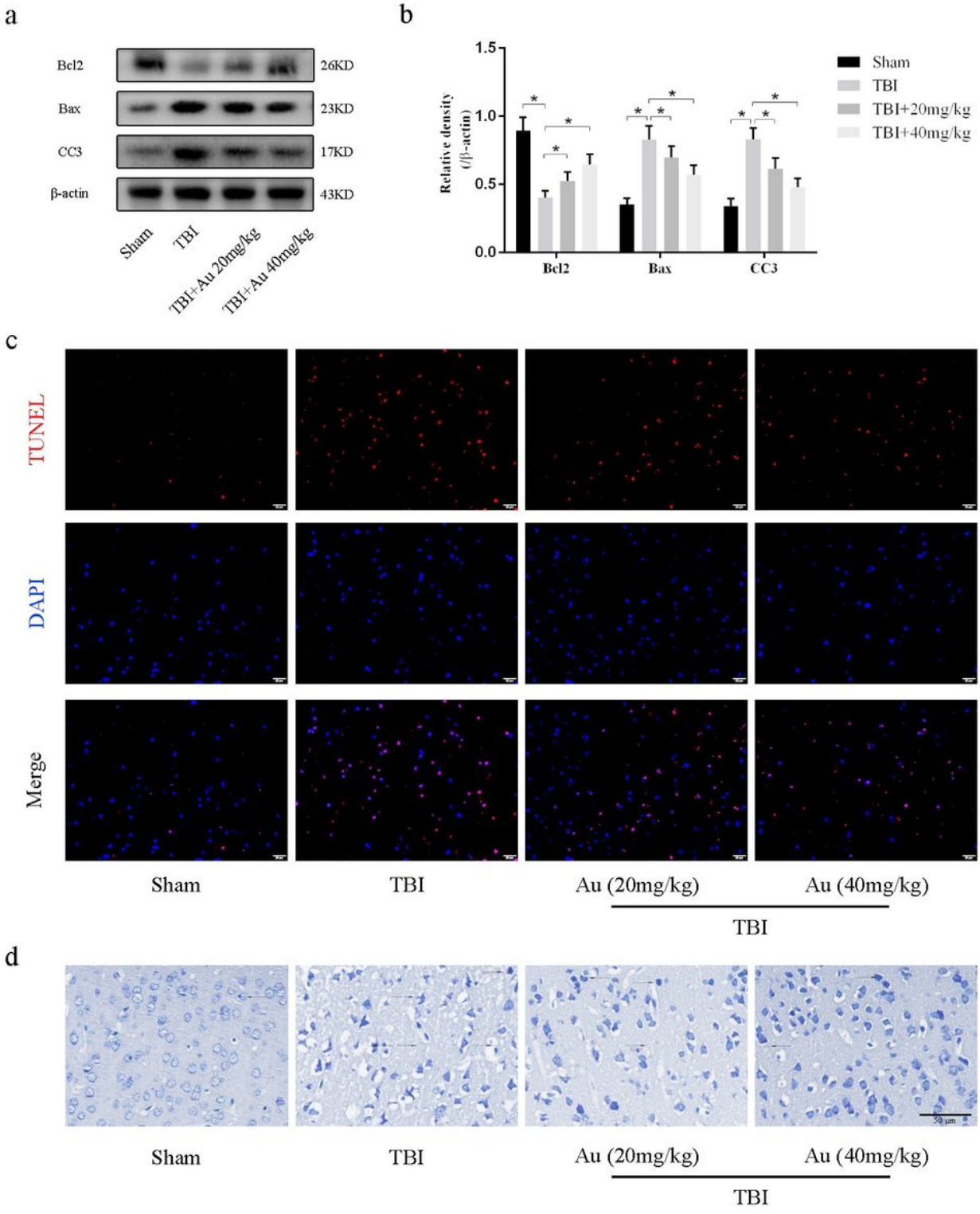

Figure 3

Au decreased the neural apoptosis and neuronal loss caused by TBI. (a, b) Representative WB bands (a) and quantification of relative protein expression (b) for Bcl2, Bax and CC3. (c, d) Representative photomicrographs showed TUNEL staining (c, Scale bars = 20 μm) and Nissl staining (d, Scale bars = 50 μm) in cortex of the traumatized side. The black arrow indicated damaged neurons. Bars represent the mean ± SD. *P < 0.05 versus indicated groups.

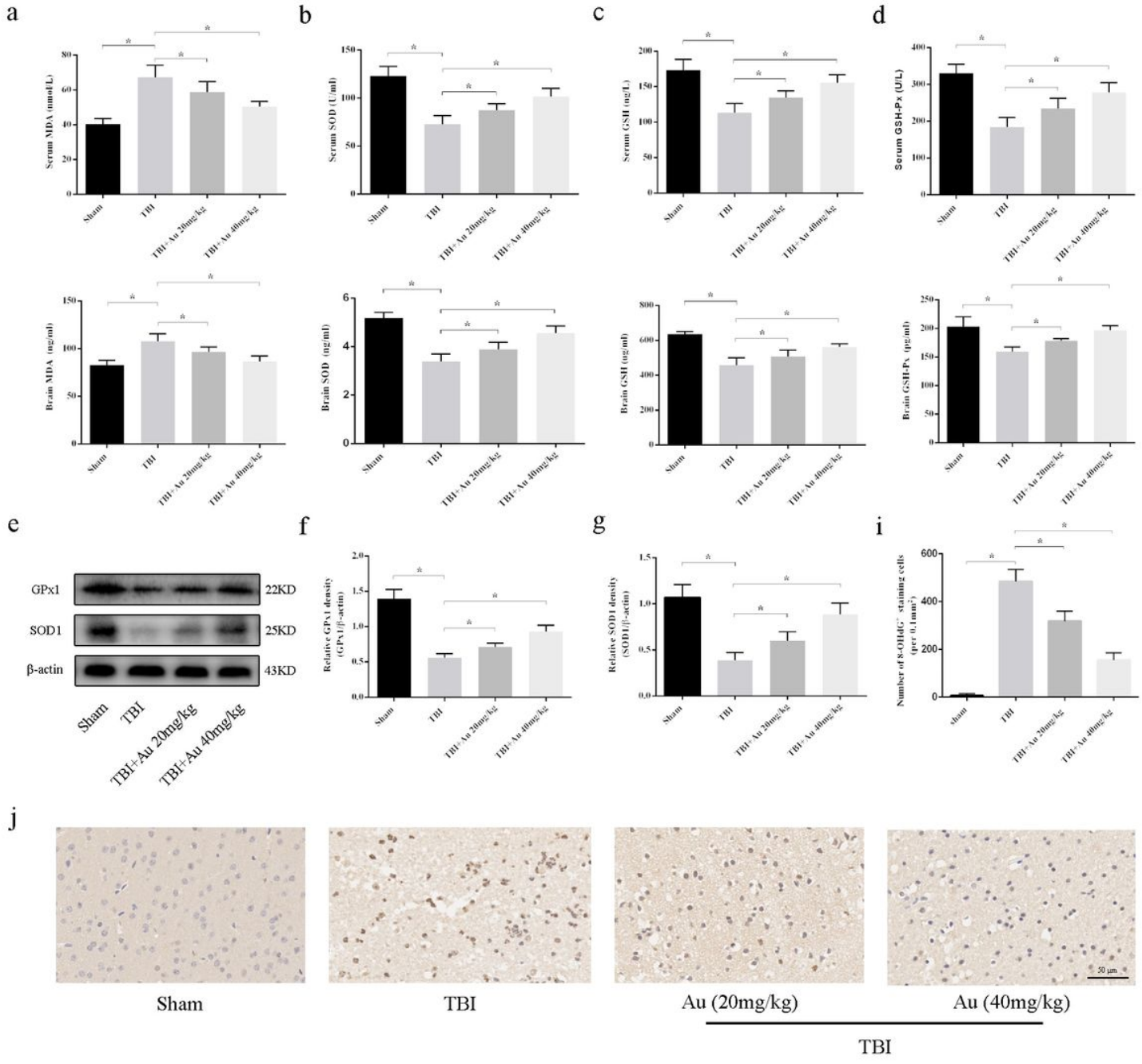

Figure 4

Au attenuates oxidative stress in TBI mice. (a-d) Au markedly decreased the level MDA (a) and increased the levels of SOD (b), GSH (c) and GSH-Px (d) in serum (upper) and brain tissue (lower) in TBI mice. (e-g) WB bands (e) and quantification of relative protein expression (f, g) for GPx1 and SOD1. (i, j)

Representative immunohistochemical images and quantitative analyses of oxidative stress markers 8-OHdG. Bars represent the mean ± SD. *P < 0.05 versus indicated groups. Scale bars = 50 μm.

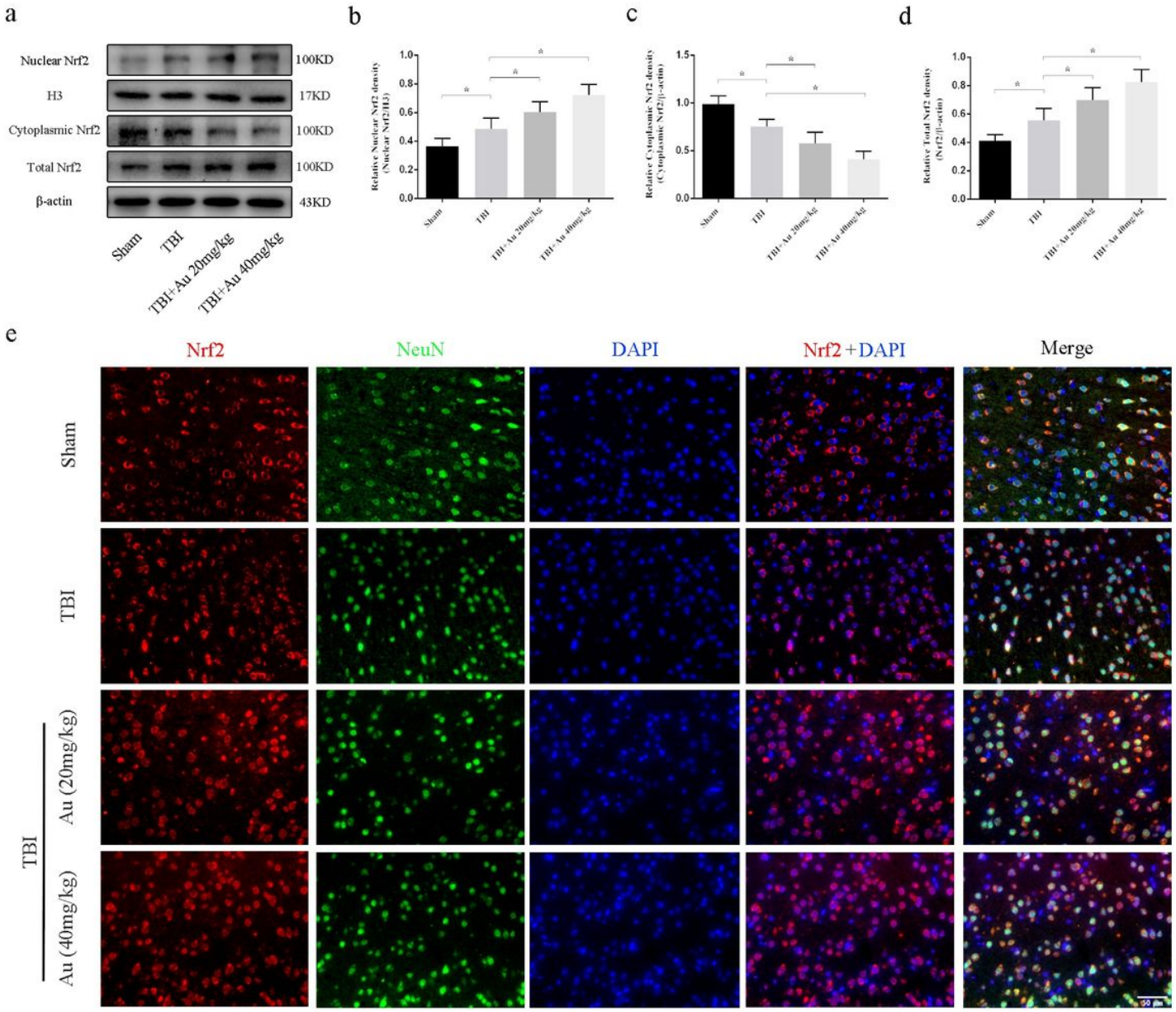

Figure 5

Effects of Au on protein level of Nrf2 in the perilesional cortex after TBI. (a-d) Representative WB bands (a) and quantification analyses of nuclear Nrf2 (b), cytoplasmic Nrf2 (c) and total Nrf2 (d). (e) Typical double immunofluorescence images of NeuN and Nrf2 (Scale bars = 50 μm). Bars represent the mean ± SD. *P < 0.05 versus indicated groups.

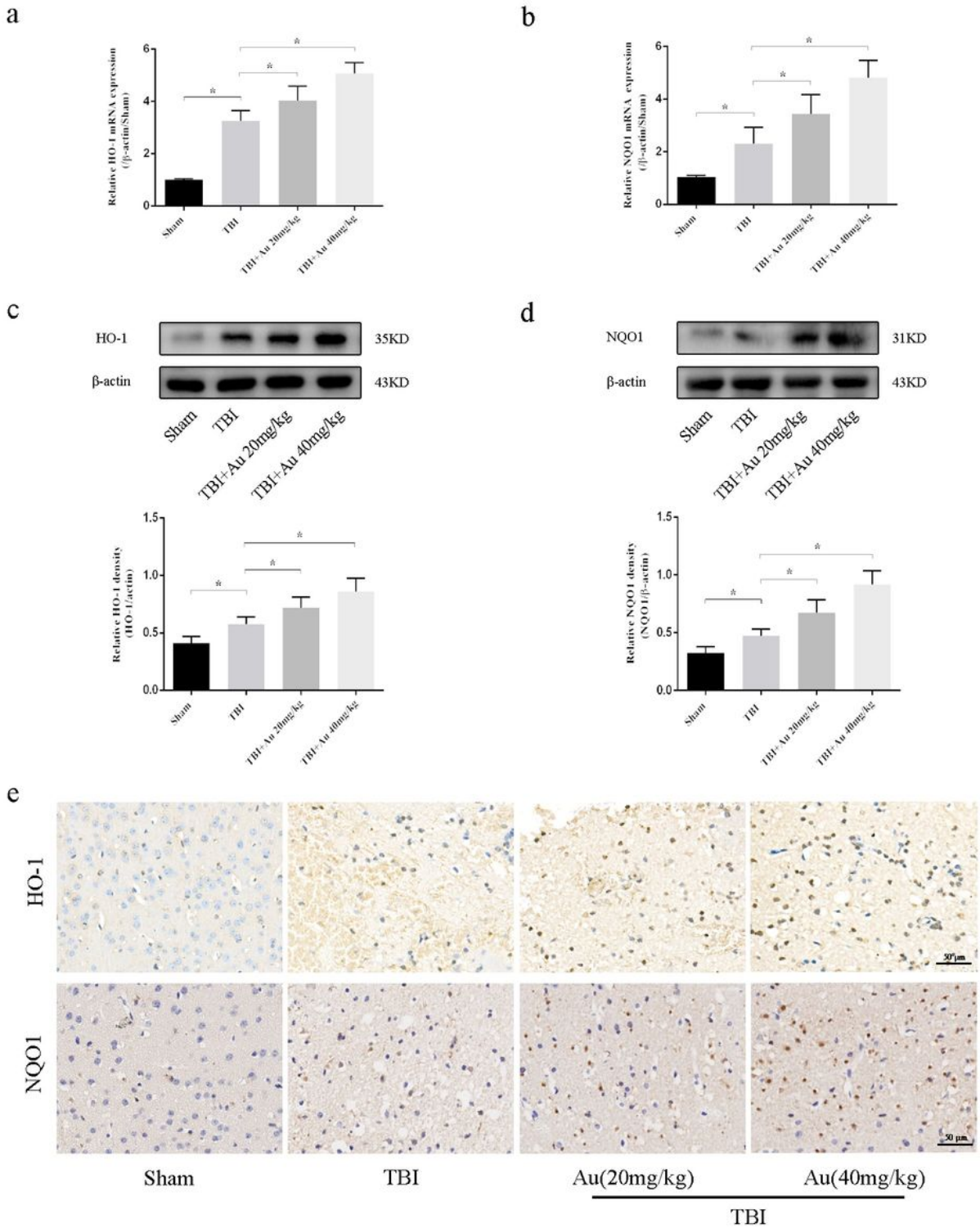

Figure 6

Au upregulated the expression of HO-1 and NQO-1. (a, b) The mRNA levels of HO-1 (a) and NQO-1 (b) in Cerebral cortex of the injured side. (c, d) WB bands (top) and quantitative analysis (bottom) of HO-1 (c) and NQO1 (d). (e) Representative IHC images of HO-1 (upper) and NQO-1 (lower). Bars represent the mean ± SD. *P < 0.05 versus indicated groups. Scale bars = 50 μm.

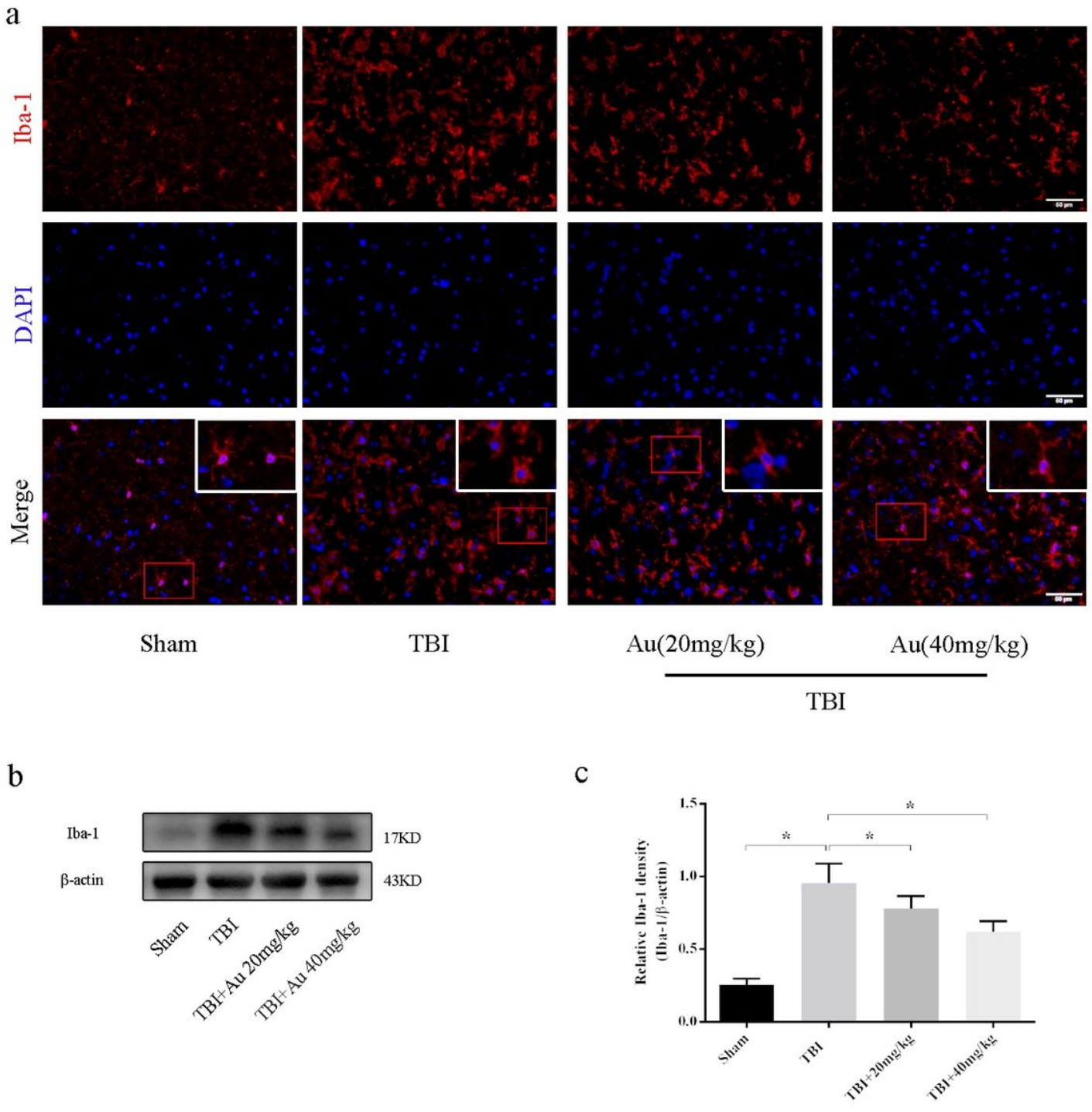

Figure 7

Effects of Au on the number of Iba-1+ cells in the perilesional cortex after TBI. (a) Representative photomicrographs showed Iba-1-positive cells in the perilesional cortex. (b, c) Representative western blot bands (b) and quantification analyses of Iba-1 (c). Bars represent the mean ± SD. *P < 0.05 versus indicated groups. Scale bars = 50 μm.

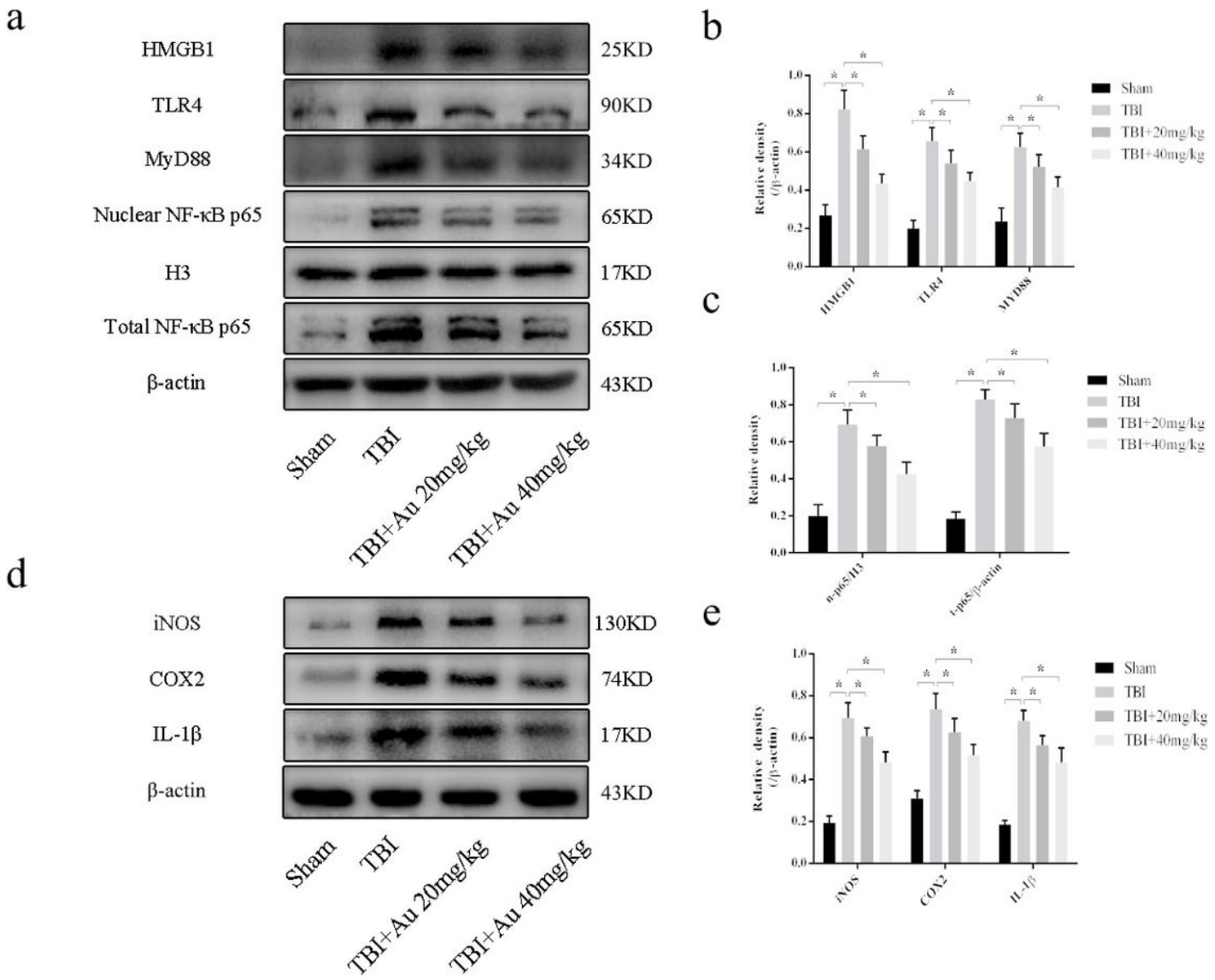

Figure 8

Au reduced HMGB1-meditated inflammation after TBI. (a-c) Representative western blot bands (a) and quantification analyses of HMGB1, TLR4, MyD88 (b), nuclear NF-κB p65 and total NF-κB p65 (c). (d, e) Representative western blot bands (d) and quantification analyses (e) of iNOS, COX2 and IL-1β. Bars represent the mean ± SD. *P < 0.05 versus indicated groups.

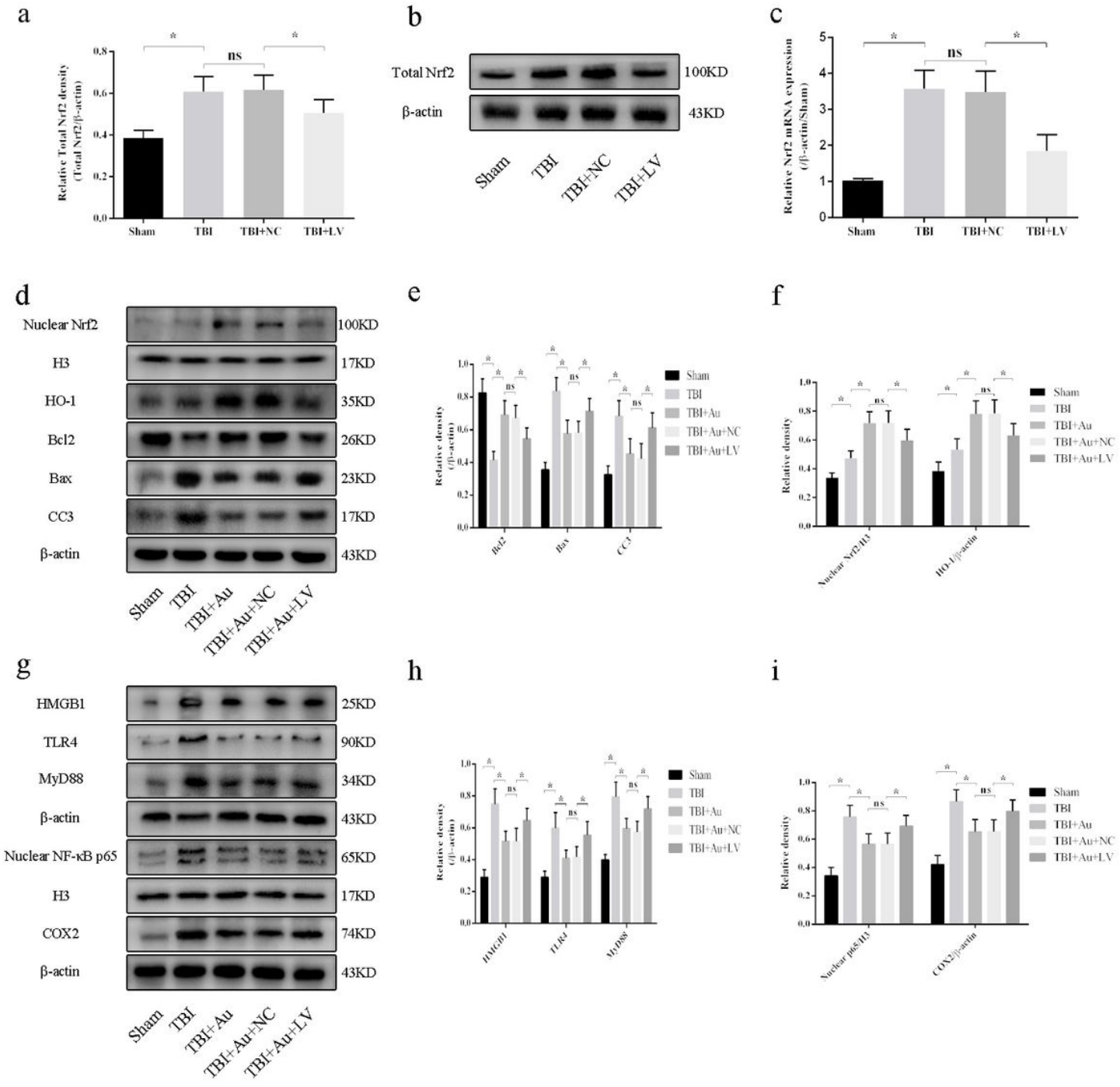

Figure 9

Effects of Nrf2 shRNA delivery and Nrf2 shRNA with Au co-administration in TBI mice. (a) The mRNA expression levels of Nrf2 in sham, TBI, TBI + NC, and TBI + LV groups. (b, c). WB assay (b) and quantification (c) of Nrf2 protein in all groups. (d-i) Representative western blot bands (d, g) and quantification analyses of nuclear Nrf2, HO-1, Bcl2, Bax, CC3 (e, f), HMGB1, TLR4, MyD88, nuclear NF-κB p65, and COX2 (h, i). Bars represent the mean ± SD. *P < 0.05 versus indicated groups; ns, not significant.